ISSN 1808-8546 (ONLINE) 1808-3765 (CD-ROM)

SENSORIAMENTO REMOTO APLICADO AO MANEJO DA IRRIGAÇÃO EM ÁREAS COM ESCASSEZ DE DADOS: ESTUDO DE CASO EM PIVÔ CENTRAL EM ITATINGA-SP*

PEDRO HENRIQUE JANDREICE MAGNONI[1]; CÉSAR DE OLIVEIRA FERREIRA SILVA[1] E RODRIGO LILLA MANZIONE[2]

[1] Departamento de Engenharia Rural, Faculdade de Ciências Agronômicas, Universidade Estadual Paulista", Avenida Universitária, n° 3780, Altos do Paraíso, 18610-034, Botucatu, São Paulo, Brasil, pedrohjmagnoni@gmail.com; cesaroliveira.f.silva@gmail.com.
[2] Departamento de Engenharia de Biossistemas, Faculdade de Ciências e Engenharia, Universidade Estadual Paulista "Júlio de Mesquita Filho", Rua Domingos da Costa Lopes, 780, CEP 17602496, Tupã – SP, Brasil. E-mail: lilla.manzione@unesp.br.
**Este artigo é proveniente das dissertações de mestrado dos dois primeiros autores.*

1 RESUMO

Ferramentas baseadas em sensoriamento remoto possibilitam o monitoramento do balanço hídrico da água em diferentes resoluções espaciais e temporais. Ainda assim, modelos que exigem dados in-situ impossibilitam sua aplicação em áreas com escassez de dados. No sentido de lidar com esse desafio, o presente trabalho apresenta uma abordagem de escolha do momento de irrigar, pelo balanço hídrico da água no solo, baseada em estimativa da evapotranspiração real (ET_A) obtida com o uso conjunto de imagens multiespectrais do sensor MSI/SENTINEL-2 e dados de uma estação meteorológica pública. A área de estudo foi um pivô central localizado no munícipio de Itatinga-SP. Para a tomada de decisão do momento de irrigar, com base em um manejo por lâmina de irrigação fixa, foi feita a interpolação da fração evapotranspirativa entre os dias com imagens disponíveis para obter a ET_A nos dias sem imagens por meio do seu produto com a evapotranspiração de referência. Essa abordagem captou variações climáticas essenciais para a estimativa do balanço hídrico em dias sem imagem. Destaca-se nessa aplicação conjunta sua capacidade de ser realizada sem necessitar de parâmetros específicos da cultura, do microclima ou do relevo, tornando-se interessante para regiões com escassez de dados.

Palavras-chave: evapotranspiração, momento de irrigar, agriwater.

MAGNONI, P. H. J.; SILVA, C. O. F.; MANZIONE, R. L.
REMOTE SENSING APPLIED TO IRRIGATION MANAGEMENT IN AREAS WITH LACK OF DATA: A CASE STUDY IN A CENTRAL PIVOT IN ITATINGA-SP

2 ABSTRACT

Remote sensing-based tools allow the monitoring of water budgets over different spatial and temporal resolutions. Nevertheless, some models require in situ data, preventing their application in areas with a lack of data. To address this challenge, this work presents an approach for irrigation scheduling, based on soil water budget estimation using actual

Recebido em 16/11/2020 e aprovado para publicação em 30/11/2021
DOI: http://dx.doi.org/10.15809/irriga.2021v1n3p585-598

evapotranspiration (ET_A) obtained using MSI/SENTINEL-2 multispectral images and data from a public meteorological station. The study area consisted of a central pivot located in the municipality of Itatinga-SP, Brazil. For decision-making of irrigation scheduling, considering a fixed irrigation rate, the evapotranspiration fraction was interpolated between the days with available images to obtain the ET_A on the days without images using its product with the reference evapotranspiration. This approach captured essential climate variations for estimating the water budget on non-image days. Noteworthy in this joint application is its suitability to be performed not requiring crop-, microclimate- or relief-specific parameters, making it useful for regions with a lack of data.

Keywords: evapotranspiration, irrigation scheduling, agriwater.

3 INTRODUCTION

The distribution of areas with proper irrigation (without considering fertigated areas) in Brazil totals 5.3 million hectares equipped for irrigation, with crops on central pivots representing 27% of the total area (National Water Agency, 2021). Although the first central pivot was only implemented in 1979, this system was responsible for almost 40% of the annual increase in irrigation systems in the last two decades (National Water Agency, 2019). For this expansion of the irrigated area throughout the country to be sustainable, it is necessary to implement irrigation management practices.

One of the sustainable irrigation management practices is correct decision-making regarding the timing of irrigation. This process is based on the cycle, crop evapotranspiration, and instantaneous soil water availability. Therefore, the soil water balance is a good indicator of this decision (GOMES, 2013). The net irrigation interval can be determined on the basis of a fixed net depth based on local climate conditions and crop characteristics, where a fixed depth is determined to replenish the soil at a rate corresponding to the accumulated water consumption over a variable period, or a fixed irrigation schedule, which corresponds to the determination of a fixed time interval for irrigation at the same frequency (CONCEIÇÃO, 2005; GOMES, 2013). By monitoring the water balance through inputs (rainfall and irrigation) and outputs (crop or actual evapotranspiration), it is possible to decide when to irrigate on the basis of the net irrigation interval.

The water balance is a relationship between inputs and outputs of the water–plant-soil system, and its components can be estimated in various ways via models that use different input variables. Therefore, the choice of modeling strategy can be limited by data availability. To address this challenge, remote sensing tools, particularly those based on images obtained by multispectral sensors on orbital satellites, can be applied to model hydrological parameters of the water balance in regions with scarce in situ data (MAGNONI; SILVA; MANZIONE, 2020). Silva; Manzione; and Albuquerque Filho (2019a) reviewed remote sensing products for irrigation management, discussing current products and platforms within this line of research. One of the potential benefits of using geospatial tools is the integration of monitoring with field actions. For example, for applications in water allocation for irrigation and the development of agricultural calendars, real evapotranspiration data obtained through modeling with satellite images make it possible to monitor the water balance and soil water availability to anticipate and mitigate water stress events

(BASTIAANSSEN; HARSHADEEP, 2005).

In Brazil, the National Water Agency (ANA) launched an unprecedented study to estimate real evapotranspiration through the automation of the Operational Model Simplified Surface Energy Balance (SSEBop) (SENAY, 2018) using Google Earth Engine, a cloud computing tool for processing geospatial data (AGÊNCIA NACIONAL DE ÁGUAS, 2020). This product is generated for the entire Brazilian territory, uses multispectral images from the OLI/LANDSAT-7 and OLI/LANDSAT-8 sensors, and is a proposal to address the lack of data on evapotranspiration.

This article proposes a decision-making strategy for irrigation timing, aimed at regions with scarce data, on the basis of the use of $ET_{modeling}$ via remote sensing together with agrometeorological data.

4 MATERIALS AND METHODS

4.1 Study area

The study area constitutes a pivot located in the municipality of Itatinga, SP. The climate in the region, according to the Köppen climate classification (1936), is defined as tropical highland (Cwa) with rainy summers and dry winters. The pivot evaluated has approximately 50 ha and is located at latitude 23° 4' 26.67" S and longitude 48° 45' 2.65" W, a rural area of the municipality, as indicated in Figure 1.

Figure 1. The study area is located in the municipality of Itatinga-SP.

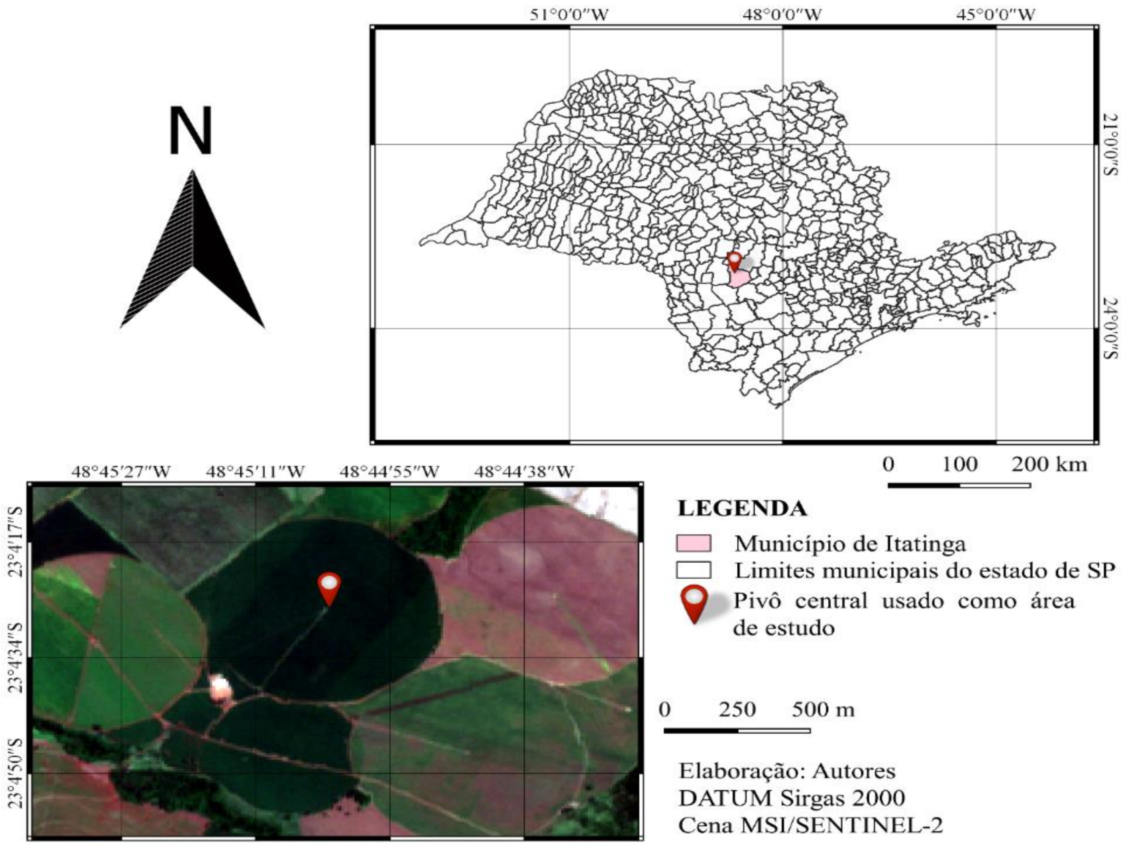

4.2 Data used

For processing satellite images and applying SAFER, the agriwater package developed by Silva; Teixeira; Manzione (2019) in the R programming language environment was used. Through this package, a user can, among other components of the energy balance, estimate the evapotranspiration fraction (ET_A / ET_o) and the ET_A spatialized for images from the OLI/LANDSAT8, MODIS/TERRA, MODIS/AQUA, and MSI/SENTINEL-2 sensors/satellites associated with data from one or more meteorological stations. The input data are a shapefile mask of the study area; reference evapotranspiration (ETo), global solar radiation (RG), and mean air temperature (TA) datasets; and reflectances from the SENTINEL-2 or TERRA/AQUA satellites or digital numbers from LANDSAT-8.

agriwater package, six MSI/SENTINEL-2 scenes corresponding to the dates of available cloud-free images were used: 2019-01-10 (Julian day (DJ) 10), 2019-01-30 (DJ 30), 2019-02-09 (DJ 40), 2019-03-26 (DJ 85), 2019-04-20 (DJ 110), and 2019-05-05 (DJ 125). Multispectral images were obtained free of charge from the USGS Earth Explorer website (UNITED STATES GEOLOGICAL SURVEY, 2013).

A public meteorological station, part of the Itatinga Forest Sciences Experimental Station (located at latitude 23° 2' 50.62" S and longitude 48° 38' 18.77" W), approximately 11 km away from the study area, provided data on global solar radiation (RG), mean air temperature (T_A) and reference evapotranspiration (ET_o) used in association with information from the MSI/SENTINEL-2 multispectral bands for $ET_{A\ modeling}$.

4.3 Modeling actual evapotranspiration (ET_A)

Remote sensors on orbiting satellites detect electromagnetic radiation reflected and emitted by the Earth's surface and atmosphere, which is interpreted in the electromagnetic spectrum according to wavelength. These data are available in raster files and require numerical processing to be interpreted in environmental and agronomic assessments, such as $ET_{A\ modeling}$. The main components of the simple model algorithm for evapotranspiration retrieval (SAFER) are surface albedo (α_0), surface temperature (T_{sup}), and the normalized difference vegetation index (NDVI). To obtain these components, a series of calculations is required per pixel, starting with the conversion of reflectances into albedo values.

The surface albedo (α_0) was estimated via Equation (1) via the coefficients proposed by Silva; Teixeira; Manzione (2019) for bands 2, 3, 4 and 8 of the MSI/SENTINEL-2 sensor:

$$\alpha_0 = b\alpha_P + c \quad (1)$$

where b and c are regression coefficients, which for a 24-hour period were considered to be 1.70 and 0.13, were obtained from field and satellite measurements (TEIXEIRA *et al.,* 2008; TEIXEIRA *et al.,* 2014a; TEIXEIRA *et al.,* 2014b) and were calibrated with $R^2 = 0.96$ (TEIXEIRA, 2010). The planetary albedo (α_P) was obtained with a weighting (Equation 2) of the reflectances in the visible and near-infrared spectra via the coefficients proposed by Silva; Teixeira; Manzione (2019):

$$\alpha_P = \sum w_{band} r_{band} \quad (2)$$

The NDVI is obtained from Equation 3:

$$NDVI = \frac{\alpha_{P_{(NIR)}} - \alpha_{P_{(RED)}}}{\alpha_{P_{(NIR)}} + \alpha_{P_{(RED)}}} \quad (3)$$

where $\alpha_{P_{(NIR)}}$ and $\alpha_{P_{(RED)}}$ represent the reflectances along the wavelengths of the near-infrared (NIR) and red (RED) regions within the solar spectrum, respectively.

To obtain the surface temperature (T_{sup}), the residual method was used (SILVA; MANZIONE; ALBUQUERQUE FILHO, 2018), presented by Equation (4):

$$T_{sup} = \sqrt[4]{\frac{\varepsilon_A \sigma T_A^4 - a_L \tau_{sw}}{\varepsilon_S \sigma}} \quad (4)$$

where ε_A and ε_S represent the atmospheric and surface emissivities, respectively, a_L represents the regression coefficient of the longwave radiation net, whose mathematical development is available in Silva; Teixeira; Manzione (2019); τ_{sw} represents the atmospheric transmissivity (considered 44% of the global solar radiation, R $_G$); T_A represents the average air temperature over 24 hours of measurement; and σ represents the Stefan–Boltzmann constant ($5.67 \cdot 10^{-8}\ W\ m^{-2}\ K^{-4}$). Equation (4) is a term-reduced version derived from the residual method based on the radiation net by the Slob equation presented in Teixeira *et al.* (2014b).

The ratio between ET $_A$ and ET $_o$, called the evapotranspiration fraction, was calculated via Equation 5 (TEIXEIRA, 2010):

$$\frac{ET_A}{ET_o} = exp\left[\mathrm{e} + \mathrm{f}\left(\frac{T_{sup}}{\alpha_0 \cdot NDVI}\right)\right] \quad (5)$$

where α_0 corresponds to the surface albedo, T_{sup} is the surface temperature, and e and f are regression coefficients of 1.8 and -0.008, respectively, following Silva; Manzione; and Albuquerque Filho (2018). Studies in other regions have successfully used other coefficients that better suit local climatic and environmental conditions, such as Hernandez *et al.* (2014) and Coaguila *et al.* (2017), who used a = 1 in the northwestern region of São Paulo. Notably, these coefficients are not fixed when the agriwater package is used, making it possible to calibrate these coefficients according to measured ET $_A$ data and perform sensitivity analyses (SILVA; TEIXEIRA; MANZIONE, 2019).

From obtaining ET $_A$/ET $_O$, ET $_A$ is obtained via Equation (6):

$$ET_A = \frac{ET_A}{ET_o} ET_o \quad (6)$$

ET $_A$/ET $_o$ in irrigated crops, such as center pivots, without environmental and water stress, can be approximated by the crop coefficient (K $_C$) (ALLEN *et al.,* 1998). In natural vegetation, the evapotranspiration fraction indicates the degree of moisture in the plant root zone and can be used to characterize water stress conditions (TEIXEIRA *et al.,* 2017; SILVA; TEIXEIRA; MANZIONE, 2019). One of the advantages of using the SAFER model, compared with the “surface energy balance algorithm for land” (SEBAL) and “mapping evapotranspiration at high resolution with internal calibration” (METRIC), is that it does not require microclimate parameters such as wind speed (at 2 m) and relative humidity as input data or a digital terrain model and the definition of “hot” and “cold” pixels; that is, it is also not necessary that in the same satellite image, there are two points with extreme and opposite water conditions (SILVA; TEIXEIRA; MANZIONE, 2019; SILVA; MANZIONE; ALBUQUERQUE FILHO, 2019b).

Since MSI/SENTINEL-2 has a temporal resolution of approximately 5 days, we applied a linear interpolation of the ET $_A$ / ET $_{o\ or\ fraction}$ on days without images, within the satellite revisit time interval, for its application in Equation 6 with measured ET $_o$ data, to obtain ET $_A$ on days without available images. This principle has already been applied to interpolate ET $_A$ on days without images in the work of Silva; Manzione and Albuquerque Filho (2019a).

Figure 2 shows the steps for calculating the estimated evapotranspiration fraction (ET $_A$/ET $_o$) via the SAFER model and its conversion to ET $_A$ via the agriwater package, from calculating the planetary albedo to obtaining the evapotranspiration fraction.

Figure 2. Flowchart for estimating ET $_A$ / ET $_o$ and ET $_A$ by applying the SAFER algorithm in the agriwater package.

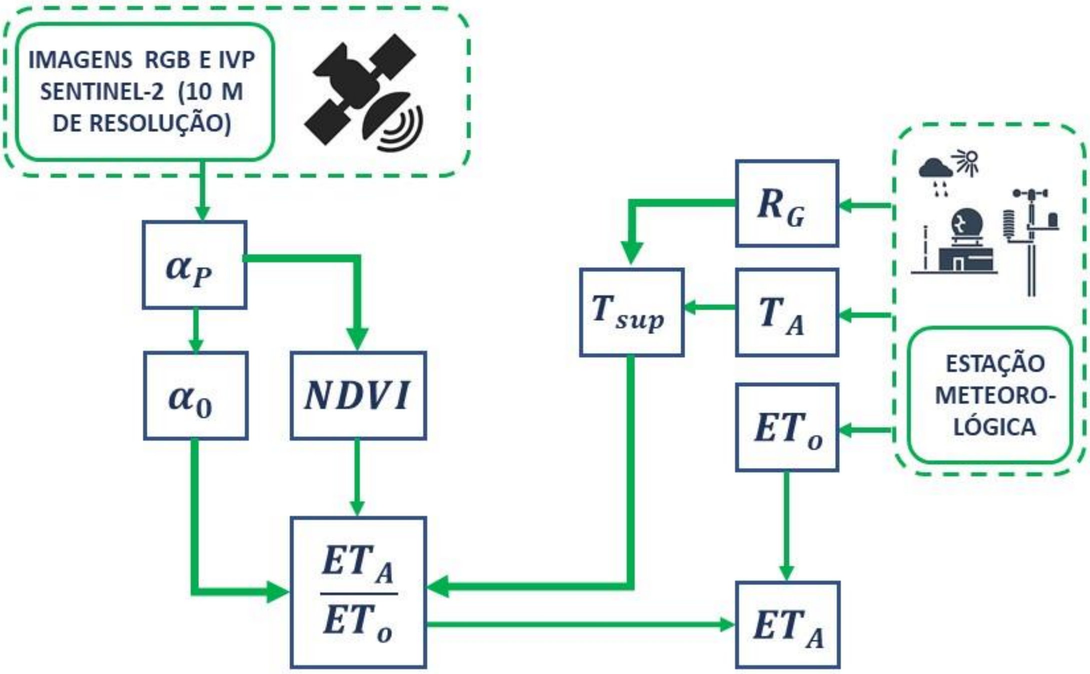

4.4 Approach to decision-making when to irrigate

Taking a fixed water depth or irrigation shift as a limit, from the moment a water deficit is detected, irrigation can be carried out to meet the demand (CONCEIÇÃO, 2005). The soil water balance has as its main components actual or crop evapotranspiration (as the main water output from the water–soil–plant system) and precipitation (as the main input). Thus, the spatialized daily balance of water consumption (C) was first determined by the difference between ET $_A$ and precipitation (Prec) at the pivot location, following Equation 7:

$$C = ET_A - Prec \quad (7)$$

To simulate the application of the methodology in a practical situation, by modeling the ET $_A$ / ET o for DJ 10, the ET A from DJ 11 to 20 was extrapolated with the respective ET $_o$ data. obtained from the meteorological station. Then, considering management with a fixed irrigation depth of 20 mm (hypothetical value), the need for net irrigation was calculated as the sum of C on a daily scale until the threshold (20 mm) was reached, which was considered the time at which irrigation was carried out.

5 RESULTS AND DISCUSSION

5.1 agrometeorological data

Figure 3 shows the weather conditions from the beginning of January 2019 (DJ 1) until June 31 (DJ 180).

Figure 3. Climatic conditions of precipitation (Prec), solar radiation (R_G), average temperature (T_A) and reference evapotranspiration (ET_o) measured at the meteorological station.

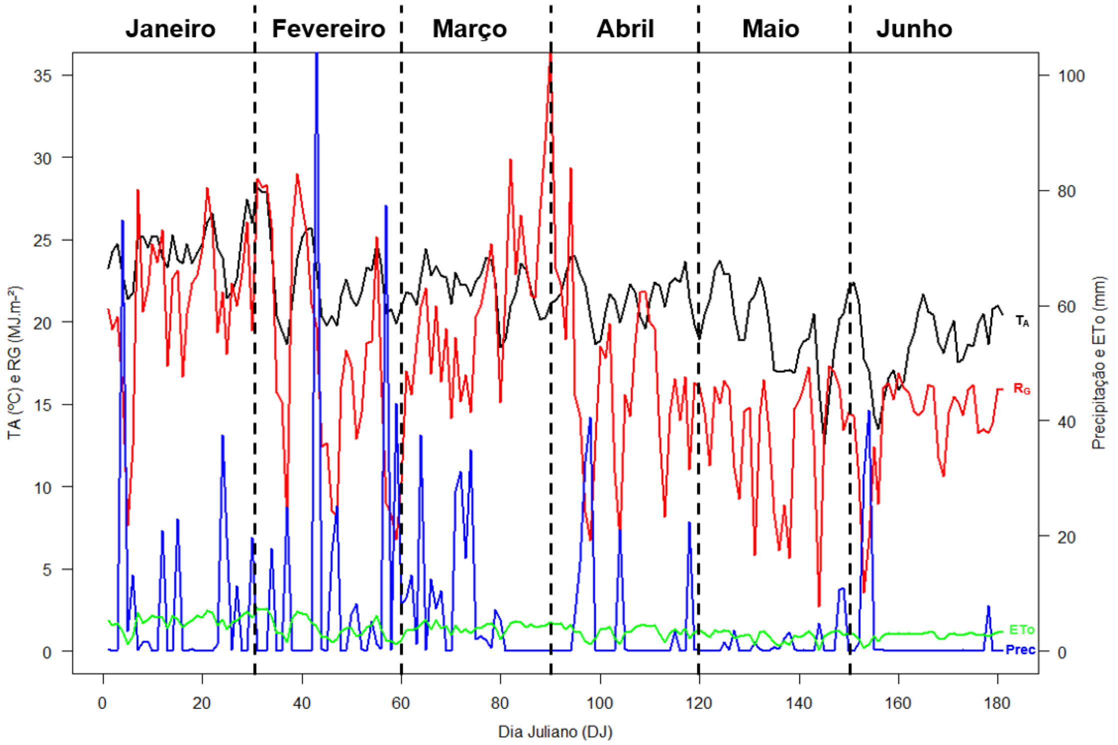

Precipitation (Prec) and global radiation (RG) data presented the greatest variability during the study period. With the exception of May, the other months presented a positive water balance between precipitation and reference evapotranspiration. Table 1 presents the maximum, minimum, and average monthly values of the agrometeorological variables monitored by the automatic station.

Table 1. Cumulative monthly maximum, minimum and average values of the variables monitored from January to June 2019.

	T_A (°C)	R_G (MJ.m $^{-2}$)	Prec (mm)	ET_o (mm)
Maximum	24.33	664.83	343.01	162.78
Minimum	18.53	402.56	40.86	81.36
Average	21.40	517.33	178.05	110.83

5.2 Modeling actual evapotranspiration

Figure 4 shows the spatial distribution of the evapotranspiration fraction at the central pivot at different DJs of the MSI/SENTINEL-2 scenes. Notably, the modeling was performed in the entire satellite scene, and subsequently, the central pivot was cut out.

Table 2 presents the means and standard deviations of ET_A/ET calculated in the pivot crop in the MSI/SENTINEL-2 scenes. These metrics were calculated after cropping to avoid the influence of pixels outside the pivot.

Figure 4. ET_A/ET_{is} estimated spatially at the central pivot.

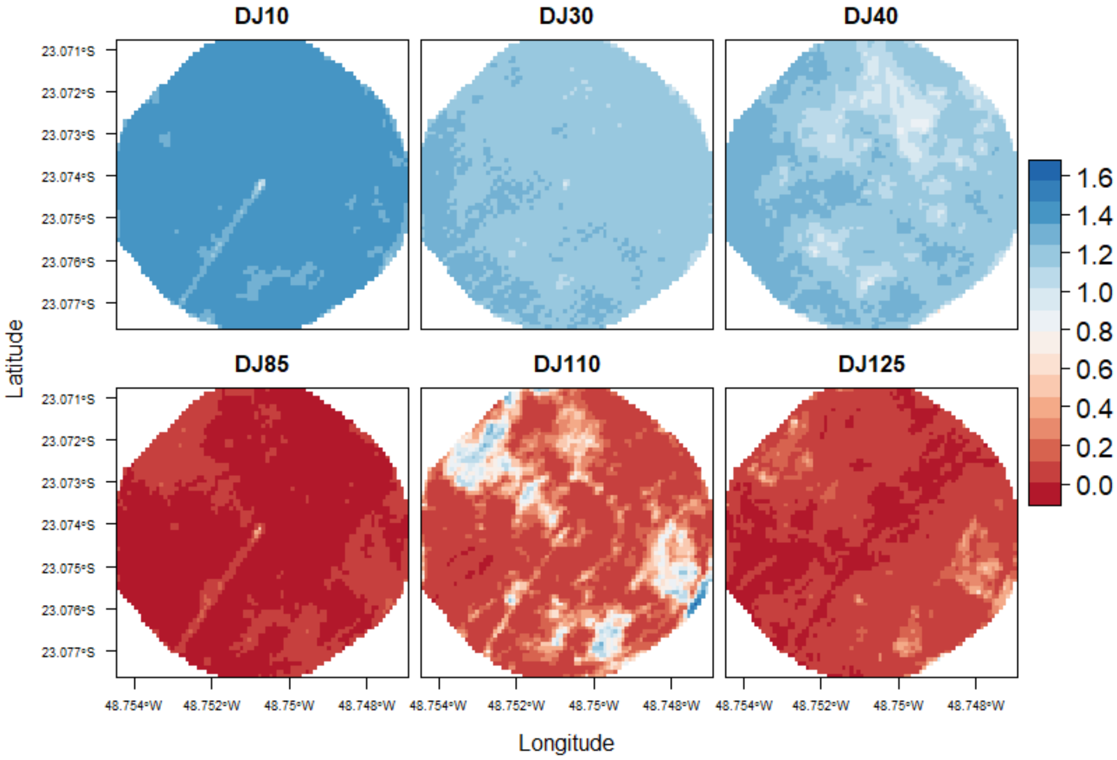

Table 2. Mean values and standard deviations of the estimated ETA/ETo in the pixels internal to the pivot point in the MSI/SENTINEL-2 scene.

DJ	Mean ± Standard Deviation
10	1.38±0.03
30	1.20±0.03
40	1.17±0.08
85	0.006±0.02
110	0.23±0.27
125	0.04±0.07

The highest ET_A/ET_o values were found at DJs 10, 30, and 40. A low standard deviation of the fraction is observed for these days, which indicates the uniformity of this parameter in the pivot. Table 2 shows a gradual reduction in the average ET_A/ET_o values from DJs 10--40. DJs 85, 110, and 125 present low ETa/ETo values since this is a period with a large amount of exposed soil.

Variation in the phenological cycle influences modeling, as different vegetative stages present distinct canopy structures that vary in surface roughness. This results in changes in wind speed that influence heat fluxes, leading to changes in reflectance and, consequently, to the modeling of evapotranspiration (FIORIO *et al*., 2018). Notably, although no specific crop parameter was considered in the modeling, the SAFER model was able to capture the temporal evolution of the plant and thus generate evidence of evapotranspiration behavior throughout the phenological phases, regardless of prior knowledge of the crop.

Figure 5 shows the interpolation of ET_A at the pivot point of DJ 11--20, obtained via Equation (6). This procedure has built-in uncertainty in the $ET_A/ET_{estimate}$ on days with available imagery. However, by using ET_{data} measured on days without available imagery, it is possible to reduce the overall uncertainty. This occurs because, using the interpolation of $ET_{A/ETo}$, analogous to K_C with measured $_{ETo}$, it is possible to capture climate variations on days without imagery, for example, in the case of rain the day after the satellite passes. This approach is less uncertain than, for example, the interpolation of ET_A because, in this case, climate variations are not captured and a linear variation is considered over the days without satellite imagery.

DJs 13 and 16 in Figure 5 were the days with the lowest daily $ET_{A\ values}$ observed during the period, both of which were estimated after the precipitation events recorded by the meteorological station at DJs 12 and 15. It is interesting to observe the effect of precipitation on the $ET_{A\ estimates}$ (in Figure 5) in the days following these events, as well as its impact on the T_A, R_G and $ET_{o\ values}$ (Table 3). If the interpolation was performed directly with the $ET_{A\ values}$, this climatic variation would not be captured since it is inserted into the modeling through the daily $ET_{o\ values}$.

Figure 5. Estimated daily ET at the pivot point between DJs 11 and 20.

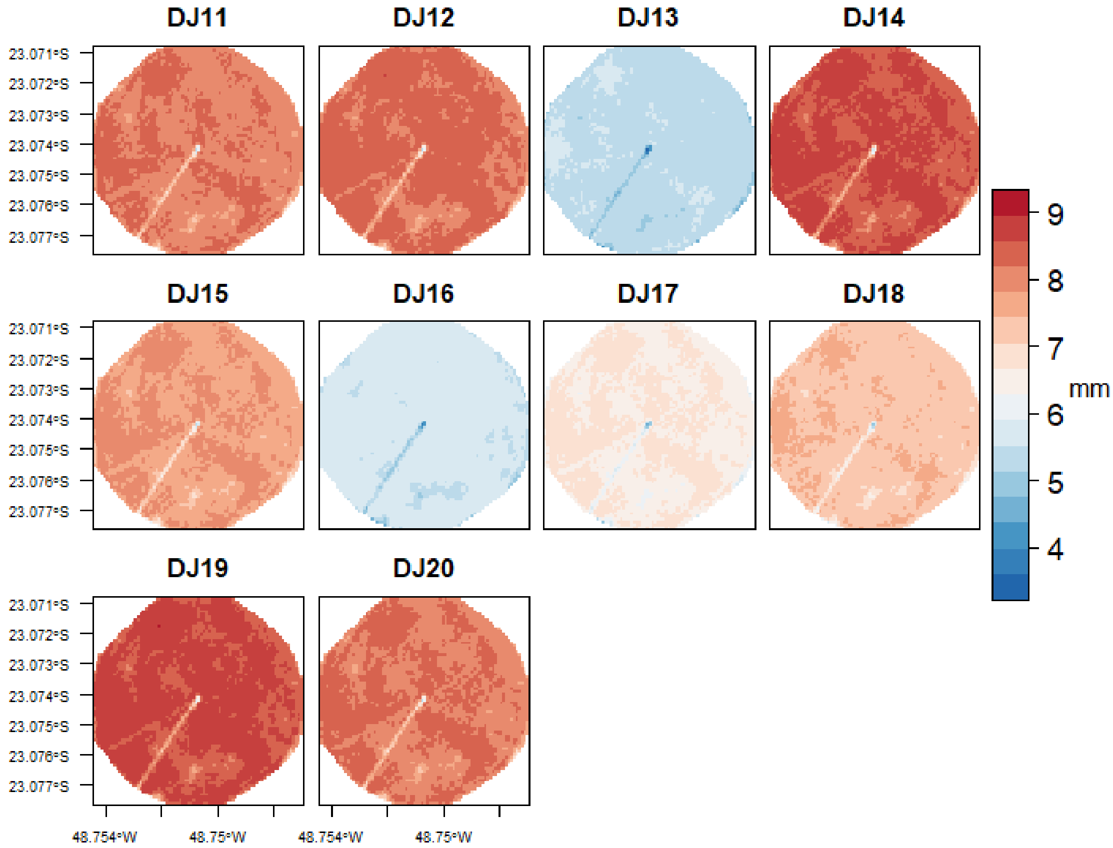

Table 3. Daily values of TA, R G, Prec and ET between DHs 11 and 20.

DJ	T_A (°C)	R_G (MJ.m $^{-2}$)	Prec (mm)	ET_o (mm)
11	25.19	23.58	0.00	5.84
12	23.92	25.56	20.87	5.92
13	23.29	17:30	0.00	3.90
14	25.29	22.65	0.00	6.15
15	23.77	23.13	22.91	5.58
16	23.54	16.68	0.15	4.06
17	24.74	20.49	0.00	4.77
18	23.56	22.36	0.29	5.27
19	24.21	22.86	0.00	6.18
20	24.74	24.43	0.00	5.86

5.3 Irrigation time

With the spatialized daily balance of water consumption (Equation 7), its evolution at the pivot point was obtained in the period between DJ 11 and 20 (Figure 6), allowing the identification of water deficit or surplus.

Figure 6. Evolution of water consumption for decision-making when irrigating.

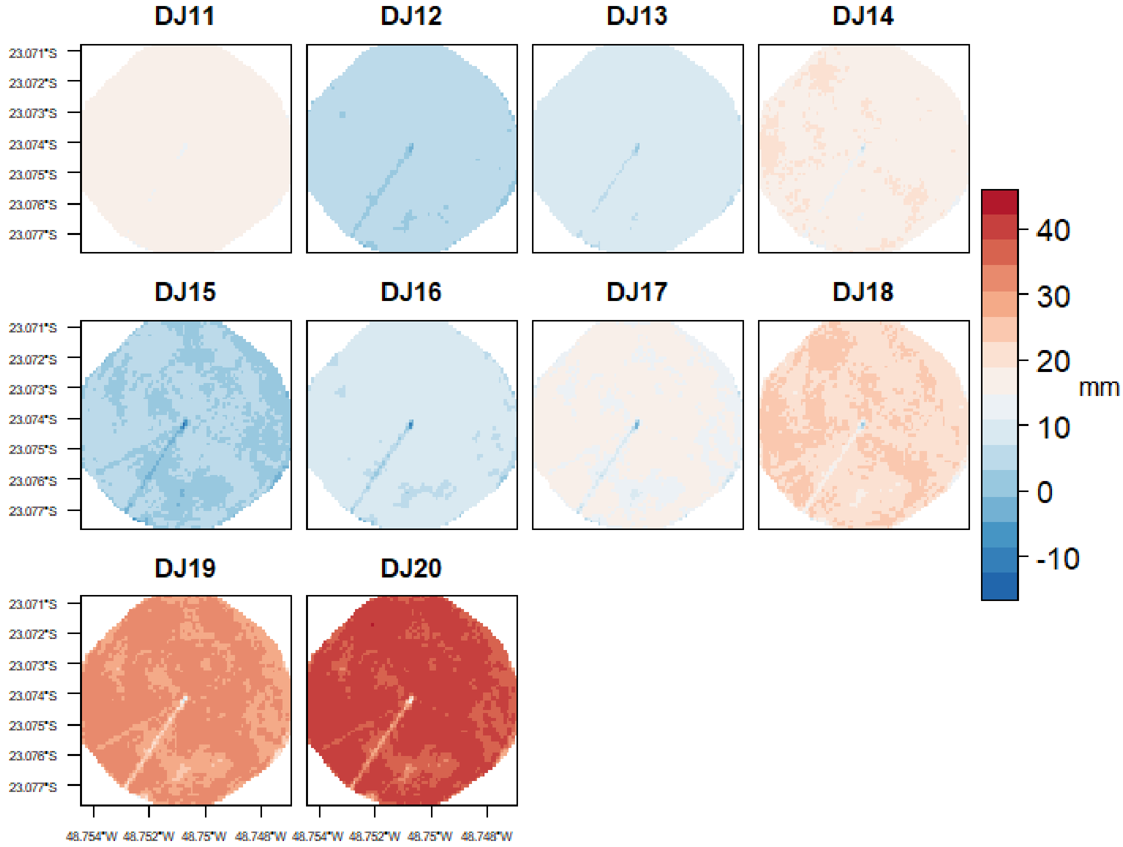

The fluctuations in accumulated ET $_A$ occur as a function of precipitation events, and when the accumulated amount exceeds the water deficit limit of the preestablished fixed depth of 20 mm, the irrigation mechanism must be activated to meet the water demand.

Despite the impossibility of validating the estimated ET $_{A\ data}$ due to the lack of data observed in the pivot, in addition to the operational difficulty in obtaining measurements of this variable, this study shows the potential for applying remote sensing to irrigation management in a spatialized manner, using multispectral images as an input source for the soil water balance, to assist in choosing the moment to carry out liquid irrigation, a procedure generally carried out on the basis of specific estimates/measurements that also present uncertainties.

6 CONCLUSION

The estimation of the water balance via daily precipitation data coupled with daily actual evapotranspiration (ET $_A$) estimated via interpolation from days with available satellite images captured local climate variations and showed the potential to guide decision-making on when to irrigate in areas with scarce data.

The potential that stands out in this joint application is its ability to be carried out without the need for specific crop, microclimate or relief parameters, making it interesting for regions with a scarcity of data.

New studies in experimental areas monitored in situ should be carried out in the future to validate this approach and promote greater safety in its practical use.

7 ACKNOWLEDGMENTS

The authors would like to thank Professors João Saad and Sérgio Campos, PhDs, for participating as a panel evaluating the qualifications of the first author in the Master's program in Agronomy – Irrigation and Drainage at FCA – UNESP/Botucatu, who contributed ideas for the subsequent development of this work. They also thank Rildo Moreira, director of the Itatinga Forest Sciences Experimental Station, for providing access to the meteorological data. They also thank the National Council for Scientific and Technological Development (CNPq) for the scholarship (Process 134361/2018-0) awarded to the first author.

8 REFERENCES

NATIONAL WATER AGENCY (Brazil). **Irrigation Atlas 2021** : Water Use in Irrigated Agriculture. 2nd ed. Brasília, DF: ANA, 2021. Available at: https://metadados.snirh.gov.br/geonetwork/srv/api/records/1b19cbb4-10fa-4be4-96db-b3dcd8975db0. Accessed on: May 7, 2021.

NATIONAL WATER AGENCY (Brazil). **Real evapotranspiration estimates by remote sensing in Brazil** . Brasília, DF: ANA, 2020. Available at: http://www.snirh.gov.br/portal/snirh/centrais-de-conteudos/central-de-publicacoes/23-estimativas-de-evapotranspiracao-real-por-sensoriamento-remoto. Accessed on: May 8, 2021.

NATIONAL WATER AGENCY (Brazil). **Survey of agriculture irrigated by central pivots in Brazil (1985-2017)** . Brasília, DF: Embrapa Milho e Sorgo, 2019.

ALLEN, RG; PEREIRA, LS; RAES, D.; SMITH, M. **Crop evapotranspiration** : guidelines for computing crop water requirements . Rome: FAO, 1998. (Irrigation and Drainage Paper, 56).

BASTIAANSSEN, WGM; HARSHADEEP, NR Managing scarce water resources in Asia: The nature of the problem and can remote sensing help? **Irrigation and Drainage Systems** , New York, vol. 19, no. 3-4, p. 269-284, 2005.

COAGUILA, DN; HERNANDEZ, FB; TEIXEIRA, AHDC; FRANCO, RA; LEIVAS, JF Water productivity using SAFER-Simple Algorithm for Evapotranspiration Retrieving in watershed. **Brazilian Journal of Agricultural and Environmental Engineering** , Campina Grande, v. 21, n. 8, p. 524-529, 2017.

CONCEIÇÃO, MAF Irrigation management. *In* : TESSMAN, DJ **Table Grape Production System in Northern Paraná** . Bento Gonçalves: Embrapa Grape and Wine, 2005. v. 10, p. 25-41.

FIORIO, PR; COELHO, RD; BARROS, PPS; BONILLA, MZ; GADY, APB Spectral behavior of sugarcane leaves in the presence of water deficit. **Irriga** , Botucatu, v. 23, n. 3, p. 609-621, 2018.

GOMES, HP **Irrigation systems** : Energy efficiency. João Pessoa : UFPB Press, 2013.

HERNANDEZ, FBT; NEALE, CMU; TEIXEIRA, AHC; TAGHVAEIAN, S. Determining large scale actual evapotranspiration using agrometeorological and remote sensing data in the northwest of São Paulo state, Brazil. **Minutes Horticulturae** , Amsterdam , v. 1038, sn, p. 263-270, 2014.

KÖPPEN, W. Das geographische System der Klimate . *In* : KÖPPEN, W.; GEIGER, R. (ed .). **Handbuch der Klimatologie** . Berlin: Gebrüder Bornträger , 1936. p. 1-44.

MAGNONI, PHJ; SILVA, COF; MANZIONE, RL Groundwater recharge and water table levels modeling using remotely sensed data and cloud-computing. **Sustainable Water Resources Management** , New York, v. 6, no. 6, p. 113, 2020.

SENAY, GB Satellite Psychrometric Formulation of the Operational Simplified Surface Energy Balance (SSEBop) Model for Quantifying and Mapping Evapotranspiration. **Applied Engineering in Agriculture** , Saint Joseph, v. 34, no. 3, p. 555-566, 2018.

SILVA, COF; TEIXEIRA, AHCT; MANZIONE, RL agriwater : An R package for spatial modeling of energy balance and actual evapotranspiration using satellite images and agrometeorological data. **Environmental Modeling & Software** , Amsterdam , v. 120, sn, p. 104497, 2019.

SILVA, COF; MANZIONE, RL; ALBUQUERQUE FILHO, JL Large-scale spatial modeling of crop coefficient and biomass production in agroecosystems in Southeast Brazil. **Horticulturae** , Basel, v. 4, no. 4, p. 44-64, 2018.

SILVA, COF; MANZIONE, RL; ALBUQUERQUE FILHO, JL Orbital remote sensing for irrigation management: a systemic review. *In* : INOVAGRI INTERNATION MEETING , 5, 2019, Fortaleza. **Proceedings** [...]. Fortaleza: INOVAGRI, 2019a. Available at: http://dx.doi.org/10.13140/RG.2.2.19266.12487. Accessed on: May 7, 2021.

SILVA, COF; MANZIONE, R.L.; ALBUQUERQUE FILHO, J.L. Comparison of SAFER and METRIC- based current evapotranspiration models in a subtropical area of Brazil . **Irriga** , Botucatu , v. 1, n. 1, Special Edition Inovagri , p. 48-55, 2019b.

TEIXEIRA, AHC ; HERNANDEZ, FBT; LOPES, HL; SCHERER-WARREN, M.; BASSOI, LH A Comparative Study of Techniques for Modeling the Spatiotemporal Distribution of Heat and Moisture Fluxes in Different Agroecosystems in Brazil. *In* : PETROPOULOS, GG (org.). **Remote Sensing of Energy Fluxes and Soil Moisture Content** . 1st ed. Boca Raton: CRC Group; Taylor and Francis, 2014a. p. 169-179.

TEIXEIRA, AHC; REIS, JBRS; LEIVAS, JF; SILVA, GBS; STRUIVING, TB Water productivity components modeled by remote sensing in irrigated lemon groves of Minas Gerais. **Agrometeoros** , Passo Fundo, v. 25, n. 1, p. 237-247, 2017.

TEIXEIRA, A. HC; BASTIAANSSEN, WGM; AHMAD, MD; MOURA, MSB; BOS, MG Analysis of energy fluxes and vegetation-atmosphere parameters in irrigated and natural ecosystems of semiarid Brazil. **Journal of Hydrology** , Amsterdam , v. 362, no. 1-2, p. 110-127, 2008.

TEIXEIRA, AHC; HERNANDEZ, FBT; ANDRADE, RG; LEIVAS, JF; BOLFE, EL Energy balance with Landsat images in irrigated central pivots with corn crop in the São Paulo State, Brazil. **Proceedings of SPIE** , Washington, DC, vol. 9239, p. 92390O-1-92390O-10, 2014b.

TEIXEIRA, AHC Determining regional current evapotranspiration of irrigated and natural vegetation in the São Francisco river basin (Brazil) using remote sensing the Penman-Monteith equation. **Remote Sensing** , Basel, v. 2, no. 5 , p. 1287-1319, 2010.

UNITED STATES GEOLOGICAL SURVEY. **EarthExplorer** . Reston: US Department of the Interior, 2013. Available at: https://earthexplorer.usgs.gov/. Accessed on: May 8, 2021.